Mapping the conformational landscape of the stimulatory heterotrimeric G protein

Robert Prosser (scott.prosser@utoronto.ca)
University of Toronto https://orcid.org/0000-0001-9351-178X
Shuya Huang
University of Toronto
Rima Rahmatullah
University of Toronto
Aditya Pandey
University of Toronto
Ned Van Eps
University of Toronto
Roger Sunahara
UCSD https://orcid.org/0000-0003-1702-8619
Oliver Ernst
University of Toronto https://orcid.org/0000-0002-8863-9444
Adnan Sljoka
https://orcid.org/0000-0002-2398-9523

Article

Keywords:

Posted Date: March 17th, 2022

DOI: https://doi.org/10.21203/rs.3.rs-1409064/v1

Abstract

Heterotrimeric G proteins serve as key membrane-associated signaling hubs, in concert with their cognate G protein-coupled receptors (GPCRs). Using site-directed labels located at four key allosteric sites within the Ras-homology domain of the stimulatory G protein α-subunit, G_sα, fluorine nuclear magnetic resonance spectroscopy (^{19}F NMR) was employed to monitor the conformational equilibria of G_sα by itself, in the intact G_sαβγ heterotrimer, or in complex with either membrane alone or membrane-embedded adenosine A_{2A} receptor (A_{2A}R). The results reveal a concerted equilibrium which is strongly affected by nucleotide and interactions with the βγ-subunit, the lipid bilayer, and A_{2A}R. ^{19}F NMR spectra of the α1 helix of G_sα exhibit significant intermediate timescale dynamics, while those associated with the α4β6 loop and the α5 helix reflect respective membrane/receptor interactions and order/disorder transitions associated with G protein activation. The αN helix adopts a key functional state that serves as an allosteric conduit between the βγ-subunit and the receptor, while spectra in the presence of GTPγS reveal that a significant fraction of the ensemble remains tethered to the membrane and the receptor upon activation.

Introduction

Heterotrimeric G proteins are membrane-anchored molecular switches that regulate intracellular signal cascades in response to activation by G protein-coupled receptors (GPCRs). The heterotrimer is composed of a nucleotide-binding α-subunit (Gα) and a dimer comprised of a β- and a γ-subunit (Gβγ). In its inactive state, Gα and Gβγ associate to form a heterotrimer (Gαβγ) where Gα is bound to guanosine diphosphate (GDP). Switching to the active state of Gα requires the exchange of GDP for GTP, which is mediated by guanine nucleotide exchange factors (GEFs) such as activated GPCRs. Here, GPCRs promote GDP release from Gα, facilitating rapid binding of guanosine triphosphate (GTP), which is present in high concentrations in the cell (Traut, 1994). GTP binding leads to functional dissociation of Gα•GTP from Gβγ and subsequent activation of downstream signaling pathways. Signaling is terminated upon hydrolysis of GTP to GDP by Gα, through its intrinsic GTPase activity or is accelerated by GTPase-activating proteins (GAPs), such as regulators of G protein signaling (RGSs). Thus, the functional ensemble of the Gα subunit is defined by conformations that enable complexation with the receptor in a GDP-bound form, the release of GDP, the binding of GTP and dissociation from Gbg, and finally the hydrolysis of GTP. Here, we use fluorine nuclear magnetic resonance spectroscopy (^{19}F NMR) to delineate these functional conformers and better understand the activation pathway.

There are four classes of Gα subunits: G_s, $G_{i/o}$, $G_{q/11}$, and $G_{12/13}$, delineated by their differing modulatory behavior on effectors. The four families share a common protein fold featuring the nucleotide binding pocket sandwiched between a Ras homology domain (RHD) and an α-helical domain (AHD). Nucleotide release requires separation of the two domains in addition to conformational changes of various switch regions that interact with the nucleotide's guanine base and phosphate groups (Chung et al., 2011; Dror et al., 2015; Van Eps et al., 2011; Westfield et al., 2011). The stimulatory family of Gα (G_sα) activates

adenylate cyclase, which produces the second messenger 3',5'-cyclic adenosine monophosphate (cAMP). High resolution structures of $G_s\alpha$ have been determined in various states along the GTPase cycle. These include GDP-bound $G_s\alpha$ in complex with Gβγ (Liu et al., 2019), nucleotide-free $G_s\alpha\beta\gamma$ heterotrimer complexed to a GPCR (Rasmussen et al., 2011), $G_s\alpha$ bound to GTPγS, a non-hydrolysable GTP analog (Sunahara et al., 1997), and $G_s\alpha$•GTPγS in complex with adenylate cyclase (Qi et al., 2019). While these structures highlight the conformational changes between different Gα states and the interaction between Gα and its binding partners, the mechanisms of GPCR-G protein complex assembly, nucleotide exchange, and dissociation of the heterotrimer have yet to be fully elucidated.

To interrogate and dissect the $G_s\alpha$ activation steps, we focused on ^{19}F-labeled $G_s\alpha$, bound to GDP, GTPγS, or a transition state analog, GDP-$[AlF_4]^-$ and we have used NMR spectroscopy to monitor the conformational equilibria and dynamics of the functional states. Each of these nucleotide conditions was applied to separate NMR studies of $G_s\alpha$ and $G_s\alpha\beta\gamma$, in addition to $G_s\alpha$ and $G_s\alpha\beta\gamma$ in the presence of a phospholipid bilayer, $G_s\alpha$ and $G_s\alpha\beta\gamma$ in the presence of a ligand-free GPCR, the adenosine A_{2A} receptor ($A_{2A}R$) and finally, in the presence of the agonist-saturated $A_{2A}R$. In this way, ^{19}F NMR spectroscopy allows us to identify key features of the conformational ensemble of $G_s\alpha$ throughout the GTPase cycle. In this study, four different labeling sites were employed to address both local and global conformational responses. The results reveal a complex landscape that is generally characterized by two global conformational signatures, one of which is selectively stabilized by membrane, Gβγ, and receptor. Each labeling site also features distinct local dynamics in response to allosteric events. Upon GTP binding, $G_s\alpha\beta\gamma$ undergoes only partial physical dissociation where some locations within $G_s\alpha$ remain in a coupled-state while others appear dissociated from Gβγ. Finally, a distinct conformational signature is observed for the αN helix of $G_s\alpha$ in the combined presence of Gβγ and $A_{2A}R$, highlighting αN's involvement in GPCR coupling and in facilitating allosteric communication between receptor and Gβγ.

Results

Labeling sites to probe the conformational dynamics of $G_s\alpha$

Previous NMR studies of G proteins have focused on $G_i\alpha$, using mainly two-dimensional ^{1}H-^{15}N or ^{13}C-methyl-based experiments (Abdulaev et al., 2006, 2005; Goricanec et al., 2016; Goricanec and Hagn, 2019; Knight et al., 2021; Ridge et al., 2006; Smrcka et al., 2010; Toyama et al., 2017). Truncation of the αN helix is common to enhance protein stability and yield. However, several studies identify strong roles of the Gα N-terminus in efficient G protein coupling and activation (Chung et al., 2011; Herrmann et al., 2006; Medkova et al., 2002). As our goals in the current investigation were to study $G_s\alpha$ in complex with the receptor and Gβγ, we regarded αN as critical to establishing a fully functional complex. Given that this compromises expression yield and protein stability, ^{19}F NMR offers an advantage since a trifluoromethyl probe provides relatively good sensitivity and protein expression can be accomplished in rich media, avoiding complicated biosynthetic labeling steps. All ^{19}F NMR studies were performed on $G_s\alpha$ using the

thiol-specific probe, 2-bromo-N-(4-(trifluoromethyl)phenyl)acetamide (BTFMA). The fluorine chemical shift is extremely sensitive to the local electronic environment and allows the delineation of conformers in the ensemble, arising from subtle changes in protein conformation and dynamics (Danielson and Falke, 1996).

To achieve site-specific labeling, we first replaced all solvent-exposed cysteine residues in $G_s\alpha$ (C3S, C200T, C237S, C359I, C365A, C379V). Similar constructs have been made previously for $G_i\alpha$ and $G_q\alpha$, and have been shown to retain native-like activity and fold (Hu et al., 2010; Kaya et al., 2014; Medkova et al., 2002). This ΔCys construct was subsequently used to generate four separate single-cysteine mutants – K34C, R61C, Y358C, and E370C (Fig. 1A). These labeling sites provide a comprehensive view of both site-specific and global conformational space of the RHD of $G_s\alpha$ without interfering with conserved sequences or switch regions that are known to play a role in receptor coupling or nucleotide exchange. We note that residue C365, which had been replaced by an alanine in the ΔCys construct, belongs to the conserved guanine-interacting TCAT/V motif. Mutation at this motif reduces the affinity of Gα for GDP, which leads to increased rates of GDP release and exchange of nucleotide (Iiri et al., 1994; Johnston et al., 2008; Posner et al., 1998; Thomas et al., 1993). We performed GTPase activity assays to assess the functionality of each $G_s\alpha$ mutant (Fig. 1F). This assay measures cumulative GTP hydrolysis in a 90-minute period, which depends on both the rate of nucleotide exchange and GTPase activity. GTP turnover is similar across all the mutants in the absence of Gβγ. In the presence of the βγ subunit, those harboring the C365A mutation exhibit enhanced GTP turnover, likely due to their reduced affinities for GDP and higher nucleotide exchange rates, consistent with previous reports. All mutants retain the ability to couple to $A_{2A}R$, as shown by increased GTP hydrolysis in the presence of agonist-bound $A_{2A}R$.

The four labeling sites are each situated at an allosterically sensitive site within the $G_s\alpha$ RHD (Fig. 1A). K34C is located on αN near the αNβ1 hinge. αN is reversibly palmitoylated in eukaryotes and helps target $G_s\alpha$ to the plasma membrane (Kleuss and Krause, 2003; Linder et al., 1993; Tsutsumi et al., 2009). It also forms part of the interaction surface with both Gβ and the receptor and becomes disordered in the absence of Gβγ (Fig. 1D). Note that the $G_s\alpha$ used in this study was recombinantly produced in *E. coli* and was therefore not lipidated. E370C is situated at the base of α5 above the conserved β6α5 loop containing the nucleotide-binding TCAT/V motif. The site is part of an ordered helix when $G_s\alpha$ is loaded with nucleotide and becomes disordered upon complexation with the receptor and nucleotide release (Fig. 1A-C). Y358C is located on the α4β6 loop at the membrane interface. This loop interacts with intracellular loop 3 (ICL3) (Rasmussen et al., 2011) and helix-8 (Hu et al., 2010) of GPCRs, making Y358C a suitable probe for assessing $G_s\alpha$ binding to the membrane or the receptor. For instance, the corresponding site in $G_i\alpha$ experiences reduced motion upon coupling to rhodopsin (Oldham et al., 2006). R61C is positioned on the α1-helix near the α1αA hinge connecting the RHD and the AHD. The site becomes disordered during receptor-catalyzed nucleotide release (Fig. 1C), making R61C a potentially sensitive probe for AHD motion and large allosteric network rearrangements within $G_s\alpha$.

We employed rigidity-transmission allostery (RTA) analysis to assess the potential for these chosen labeling sites to respond to perturbation at the $G_s\alpha$ nucleotide binding pocket. RTA is a computational method based on the mathematical rigidity theory and is used to identify allosteric networks within proteins (Jacobs et al., 2001; Sljoka, 2021; Whiteley, 2005). The algorithm was carried out on a model derived from the crystal structure of GDP-bound $G_s\alpha\beta\gamma$ (Liu et al., 2019). This involved computationally rigidifying the bound GDP, then quantifying the changes in conformational degrees of freedom across the system. The results are plotted in Fig. 2 for each residue of $G_s\alpha$, where a larger change in degrees of freedom signifies stronger allosteric transmission from the nucleotide binding site. All labeling sites except for K34 were found to be allosterically engaged to the bound GDP. The greatest allosteric transmission is observed at the phosphate-interacting P-loop (β1α1 loop) and the N-terminal portion of the α1 helix. This is consistent with recent mutagenesis studies identifying the P-loop to be most critical for stabilizing GDP binding (Ham et al., 2021), as well as bioinformatics analysis that highlighted the role of α1 as a structural hub (Flock et al., 2015).

$G_s\alpha$ undergoes global and local conformational changes as a function of membrane, Gβγ, nucleotide, and receptor

To monitor the conformational changes of $G_s\alpha$ at different stages of the GTPase cycle, we acquired ^{19}F NMR spectra of BTFMA-labeled $G_s\alpha$ as a function of Gβγ, nucleotide, membrane without receptor, and $A_{2A}R$ reconstituted in discoidal high-density lipoprotein particles (rHDLs, commonly known as nanodiscs). To create a membranous environment, empty nanodiscs were employed. The corresponding ^{19}F NMR spectra, shown in Fig. 3, generally reveal two sets of NMR resonances, denoted A and B. Interestingly, the response of the A/B equilibria as a function of condition are similar among all 4 labeling sites. In the absence of membrane and Gβγ, $G_s\alpha$ predominantly populates state A. Shifts in equilibria toward B are observed for GDP-bound or nucleotide-free $G_s\alpha$ in the presence of either membrane, Gβγ, apo $A_{2A}R$, or $A_{2A}R$ bound to the full agonist NECA. The addition of GTPγS saw a return of population A in some but not all labeling sites, suggesting a partial uncoupling of $G_s\alpha$ from the membrane or Gβγ. Taken together, the ^{19}F NMR spectra point to the presence of two broad energy basins in the conformational landscape of $G_s\alpha$ (A and B), whose equilibrium is jointly modulated by the phospholipid bilayer, the Gβγ subunit, the receptor, and nucleotides. While nucleotide binding stabilizes A, the presence of phospholipid, Gβγ, and receptor all bias the ensemble toward B.

In addition to coordinated global changes, the ^{19}F NMR spectra from the four labeling sites reveal differences in local dynamics and their response to environmental perturbation. For instance, a series of broad NMR signatures (~ 600 Hz line width) in the R61C spectra point to conformational exchange events on an intermediate (μs-ms) timescale. On the other hand, the narrower resonances (40–50 Hz) observed in the spectra of K34C suggest much faster motional averaging. Other site-specific observations are addressed below.

K34C (αN helix)

The K34C spectral series is characterized by two narrow upfield resonances at -61.72 ppm and – 61.89 ppm, and a broader downfield resonance at -60.87 ppm that only appears in the combined presence of Gβγ and $A_{2A}R$ (Fig. 3). Exchange between the two upfield peaks coincide with transitions between the two global conformational states discussed above. The K34C labeling site is located on the N-terminal helix of $G_s\alpha$, approximately one turn away from the αNβ1 hinge (Fig. 4A). This helix is mostly disordered in the absence of Gβγ, as shown by electron paramagnetic resonance spectroscopy and through missing electron densities in the crystal structures of $G_s\alpha$•GTPγS and $G_i\alpha$•GDP (Coleman and Sprang, 1998; Medkova et al., 2002; Sunahara et al., 1997). Therefore, the two upfield resonances (A and B) are likely reporting on conformational disorder/order at the labeling site, where helix formation (B) is induced upon contact with the membrane. Phospholipid binding may be facilitated through sidechains of multiple lysine residues on αN, which can form electrostatic interactions with negatively-charged lipid headgroups.

A broad downfield signature is observed for GDP-bound and nucleotide-free K34C in the joint presence of Gβγ and $A_{2A}R$, which is abolished upon the addition of GTPγS (Fig. 4B). This resonance likely represents a distinct conformation or local environment at the N-terminal helix that arises from complexation with both Gβγ and the receptor. In the structures of β_2AR-bound $G_s\alpha\beta\gamma$ and $A_{2A}R$-bound mini-G_s heterotrimer, the intracellular loop 2 (ICL2) of both receptors form a 2-turn helix that pack against the αNβ1 hinge (García-Nafría et al., 2018; Rasmussen et al., 2011). Residue K34 is located near this hinge and is “sandwiched” between the receptor and the Gβ subunit during receptor coupling (Fig. 1B & 1C). Interestingly, this “sandwiched” state constitutes a minor population of the ensemble, suggesting that αN of $G_s\alpha\beta\gamma$ remains somewhat dynamic while coupled to the receptor. The sandwiched state is abolished by GTPγS, whose addition resulted in the stabilization of two new resonances at -61.79 ppm and approximately – 62.09 ppm (Fig. 4B). The peak at -61.79 ppm could be the result of a new conformer, or a shift in the original A state through exchange averaging with the broader upfield resonance at -62.09 ppm. The resolution of these new peaks, combined with the fact that binding by GTPγS did not return the equilibrium toward the original A ($G_s\alpha$ only) state, suggest that $G_s\alpha$ is not fully dissociated from the receptor in response to GTPγS but adopts a different set of conformations compared to $G_s\alpha$•GTPγS alone (Figs. 3 & 4B).

Another possible explanation for the distinct downfield state at K34 may be related to the AHD-αN interaction that is observed in the G_s-β_2AR complex structure. In the crystal structure of the nucleotide-free state, the AHD interacts with both Gβ as well as with αN, thus stabilizing the open conformation of the $G_s\alpha$. On the other hand, structures of Gα bound to GTPgS or GDP•$[AlF_4]^-$ show an AHD-RHD closed conformation suggesting that the chemical shift at K34 may result from the proximity of AHD to αN in the apo and GDP-bound states of Gα. This effect is only observed in phospholipid, underlying the strong influence of the bilayer on the structure of αN.

R61C (α1 helix)

The spectrum of G_sα•GDP at R61C reveals a broad A state resonance that sharpens significantly upon the replacement of GDP for GTPγS (Fig. 3). The broader linewidth indicates intermediate (μs-ms) timescale conformational exchange at the labeling site, which is located on α1 near the α1αA hinge that connects the RHD and AHD (Fig. 5A). This may be a result of spontaneous domain separation, which has been shown by molecular dynamics simulations to occur on a μs-timescale in the GDP-bound G protein (Dror et al., 2015). Structural and bioinformatic analysis across the four Gα families found α1 to be an allosteric hot spot and a structural hub linking α5, GDP, and regions of the AHD (Flock et al., 2015). These contacts are lost upon receptor binding, which causes partial disordering of the α1-helix in the absence of nucleotide (Figs. 1 and 5A). The transition from state A to state B at R61C may be indicative of this loss in α1 integrity or other structural rearrangements within G_sα. The B state resonance is broad, suggesting that α1 remains dynamic and undergoes intermediate timescale motion when coupled to Gβγ or the receptor, possibly reflecting the dynamic motion of AHD.

E370C (β6α5 loop/α5 helix)

E370C is located at the end of the β6α5 loop, which connects to α5. This junction undergoes an order-to-disorder transition during receptor coupling as the C-terminal end of α5 inserts into the receptor's intracellular cavity, leading to nucleotide release (Figs. 1C and 5B) (Chung et al., 2011). The labeling site is characterized by at least three underlying resonances in the ^{19}F NMR spectra: the A state at -61.65 ppm, the B state at -61.99 ppm, and a downfield shoulder at -61.50 ppm whose population is slightly enhanced in the presence of the membrane. The A and B states may signify the labeling site being part of an ordered helix (A) or a disordered loop (B) (Fig. 5B). While the ordered helix (state A) is predominantly favored for G_sα•GDP and G_sα•GTPγS, state B is best stabilized for nucleotide-free G_sα that is coupled to the receptor. Interestingly, the presence of membrane or Gβγ also promoted the B state in addition to the downfield resonance at -61.50 ppm. This third resonance may be a consequence of the interaction between the α5 helix and the phospholipid bilayer and represents an intermediate state that is sampled prior to stable complexation with the receptor (Du et al., 2019; Kim et al., 2021; Liu et al., 2019).

Y358C (a4b6 loop)

In comparison to other labeling sites, Y358C shows a clearer delineation of nucleotide binding states. The chemical shift of state A is -61.19 ppm for G_sα•GDP and − 61.33 ppm for G_sα•GTPγS (Figs. 3 & 6A), pointing to conformational or environmental differences at the α4β6 loop where Y358C is located. The α4β6 loop is away from any nucleotide-binding elements or switch regions, with the Y358 sidechain overlaying almost completely between the G_sαβγ•GDP and G_sα•GTPγS crystal structures (Fig. 6B). However, this residue is also part of the crystal packing interface (in the G_sα•GTPgS structure), which experiences hampered conformational dynamics. The observed chemical shift sensitivity toward nucleotide in our ^{19}F NMR spectra and allosteric propensity analysis (Fig. 2) suggests that the structure of the α4β6 loop may be quite different in solution from that of the crystals. Interestingly, the chemical shift of state B is not sensitive to the identity of the nucleotide. We wondered whether state B is simply a consequence of the probe being brought in close proximity to the phospholipid bilayer via heterotrimer

assembly or receptor complexation. However, the addition of Gβγ without empty nanodiscs also shifted the equilibrium toward B, suggesting that this pose is allosterically induced and can be stabilized independently by either Gβγ or phospholipid (Figs. 3 & 6A).

G_sαβγ undergoes partial dissociation with GDP-$[AlF_4]^-$ and GTPγS

Classically, activation of the G protein by a GPCR involves GTP binding followed by subunit dissociation of the heterotrimer (Hamm, 1998). However, multiple lines of evidence suggest that the α- and the βγ-subunits do not completely dissociate upon activation (Adjobo-Hermans et al., 2011; Bünemann et al., 2003; Digby et al., 2008; Galés et al., 2006; Hillenbrand et al., 2015; Klein et al., 2000; Ridge et al., 2006; Tang et al., 2006; Wang et al., 2008). Instead, the heterotrimer undergoes structural rearrangements that would allow the α- and the βγ-subunits to remain loosely associated while interacting with their respective effector proteins (Bünemann et al., 2003; Galés et al., 2006; Kano et al., 2019; Rebois et al., 2006; Tang et al., 2006). GTPγS and GDP-aluminum fluoride (GDP-$[AlF_4]^-$) are widely used GTP analogs in the study of GTPases. GDP-$[AlF_4]^-$ is also a transition state analog for the GTP hydrolysis reaction (Wittinghofer, 1997). In the structures of GDP-$[AlF_4]^-$-bound G_iα and G_tα, the $[AlF_4]^-$ moiety occupies the space that is normally taken up by the γ-phosphate of GTP and mimics the transition state of phosphoryl transfer (Coleman et al., 1994; Sondek et al., 1994; Sprang, 2016).

We examined the effects of both GTPγS and GDP-$[AlF_4]^-$ on G_sα as a function of membrane and Gβγ. The ^{19}F NMR spectra of G_sα•GDP, G_sα•GDP-$[AlF_4]^-$, and G_sα•GTPγS show predominantly the A state for all four labeling sites in the absence of the membrane (Fig. 7). There is a general bias toward sampling of the B state for G_sα•GDP when membrane is added. GDP-$[AlF_4]^-$ and GTPγS were able to revert this effect for K34C and E370C but not for Y358C, suggesting a partial uncoupling of G_sα from the membrane by GTP analogs. In the case of R61C, a return of the sharp A state resonance is stabilized by GTPγS but not by GDP-$[AlF_4]^-$, indicating that GDP-$[AlF_4]^-$ gives rise to an intermediate of G_sα between the GDP- and GTP-bound forms. The combined presence of Gβγ and membrane further reinforced state B for all four labeling sites. While the exchange of GDP for GTPγS partially reverted this equilibrium toward state A for K34C and E370C, no change is observed for Y358C and R61C. Consistent with a transition-state analog, GDP-$[AlF_4]^-$ saw an intermediate A state population for K34C but otherwise similar spectra as G_sαβγ•GDP for E370C, Y358C, and R61C.

The above observations suggest that in the heterotrimeric form, the α- and βγ-subunits remain associated and membrane-attached throughout the GTPase cycle. The exchange of GDP for GTP triggers structural rearrangement within G_sα, leading to a partial dissociation of the heterotrimer where some portions of the α-subunit (such as the α4β6 loop and the α1 helix) remain in a coupled conformation while other locations (such as αN and α5) become decoupled. Finally, although near-identical structures were

obtained for $G_i\alpha$•GDP-$[AlF_4]^-$ and $G_i\alpha$•GTPγS in solution (Coleman et al., 1994), our NMR data indicate that in the presence of the membrane, GDP-$[AlF_4]^-$ gives rise to a conformational ensemble of $G_s\alpha$ where the relative population of each state falls between that of the GDP- and GTP-bound conditions.

Discussion

In this study, ^{19}F NMR spectroscopy was used to map the conformational landscape of $G_s\alpha$ throughout the GTPase cycle. Four distinct labeling sites were examined as a function of Gβγ, $A_{2A}R$, and nucleotides which included GDP, GTPγS, and GDP-$[AlF_4]^-$, in the presence and absence of a membrane-like environment. Two global states, A and B, were identified where transitions between them are coordinated across all four labeling sites. While the binding of a nucleotide generally stabilizes state A, the presence of phospholipid, Gβγ, and receptor all independently bias the $G_s\alpha$ equilibrium toward state B. It is conceivable that these two states reflect the crystallographic end points of $G_s\alpha$, with A representing an RHD-AHD "closed" conformation as depicted in the structure of $G_s\alpha$•GTPγS, and B corresponding to an "open" conformation, as represented by the nucleotide-free structures of $G_s\alpha\beta\gamma$ bound to GPCRs where the RHD and the AHD are maximally separated. This does not necessarily indicate a nucleotide-free $G_s\alpha$, since domain separation alone is not sufficient for GDP release (Dror et al., 2015). Regardless of the global structural interpretations of A and B, each labeling site is ultimately a probe of the local environment and is influenced differently by the nucleotides, Gβγ, and the lipid bilayer in comparison to other locations within the protein. Therefore, site-specific interpretation of the NMR spectra may provide more reliable, albeit regional, insights into the protein's conformation and dynamics under each of the given conditions. For example, the exchange line broadening observed for R61C is indicative of μs-ms timescale dynamics, potentially due to spontaneous domain separations or rearrangements of internal contact networks. The A-B transitions for K34C, R61C, and E370C may reflect changes in the conformational order/disorder at αN, α1, and α5, respectively. Y358C gave rise to a large chemical shift difference between $G_s\alpha$•GDP and $G_s\alpha$•GTPγS, revealing a clear allosteric connection from the α4β6 loop to the nucleotide binding pocket. Finally, multiple resonances are observed for K34C and E370C in addition to states A and B, which points to a more complex mechanism underlying the regulation of $G_s\alpha$.

The phospholipid bilayer appears to play a significant role in shaping the conformational landscape of $G_s\alpha$. This is not surprising for K34C, given that the $G_s\alpha$ N-terminus is generally palmitoylated and anchored to the membrane (Kleuss and Krause, 2003; Linder et al., 1993; Tsutsumi et al., 2009). Our NMR data show that αN interacts with the phospholipid bilayer in the absence of a lipid anchor. The recent structure of the dopamine D_2-G_i complex resolved in a phospholipid bilayer revealed significant electrostatic interactions between the phospholipid headgroups and the αN helix of $G_i\alpha$, in addition to their interactions with the putative acylated N-terminal lipid anchor (Yin et al., 2020). The organization of αN at the phospholipid interface may give rise to subsequent conformational changes at distal sites of the protein, thereby lowering the barrier for $G_s\alpha$ to adopt an overall conformation (e.g. state B) that is more complementary for receptor coupling. Similarly, the βγ-subunit, in addition to stabilizing the $G_s\alpha$-

membrane interaction through an additional lipid anchor on Gγ and enabling interaction with the receptor (Herrmann et al., 2006), reinforces the allosteric changes brought about by the membrane and further shift the G_sα conformational ensemble to a receptor coupling state. As seen in Fig. 3, though $A_{2A}R$ is more effective at stabilizing state B in comparison to the membrane alone, the combined effects of membrane and Gβγ are nearly equivalent to that of the receptor plus Gβγ. The exception is K34C, which revealed a distinct conformational signature in the joint presence of $A_{2A}R$ and Gβγ. This “sandwiched” state is reinforced by the $A_{2A}R$ full agonist NECA and may be indicative of the strength of receptor-G protein coupling within the ternary complex. It has recently been shown that the βγ-subunit, though not directly in contact with $A_{2A}R$, plays a role in transmitting ligand efficacy (Huang et al., 2021). This may be relayed through αN, which is held at the membrane interface between the receptor and Gβ. These NMR data are further evidence for N-terminal helix involvement in receptor coupling and its role of bridging the allosteric communication between the receptor and Gβγ. We also cannot rule out the potential contributions of the interaction between αN and the AHD in the open conformation that is stabilized in the nucleotide-free state of Gα, as revealed in the G_s•β_2AR complex structure.

We have previously shown that the activation of $A_{2A}R$ proceeds through a conformational selection mechanism (Huang et al., 2021; Ye et al., 2016). Furthermore, coupling between an apo, partial agonist-bound, or full agonist-bound $A_{2A}R$ with heterotrimeric G protein each stabilizes a distinct activation state of the receptor. We hypothesized that through reciprocal conformational selection, the G protein might also adopt distinct conformations specific to the state of the receptor and whose populations and lifetimes are determined by intrinsic ligand efficacy. This is not observed in our data with these probes, which show near identical spectra for the G protein coupled to an apo or a full agonist-bound $A_{2A}R$ (Fig. 3). Our labeling sites may not have provided the sensitivity required to resolve such conformers, being relatively distant from the receptor’s intracellular cavity. Better differentiation of the receptor states may be afforded by probes located closer to the receptor along α5, such as F376, R389, and E392 (residue 8, 21, and 24 on α5) (Kaya et al., 2014; Liu et al., 2019), provided that mutagenesis and labeling do not significantly change the nature of the interaction with receptor or the signal transmission pathway.

The current study provided strong evidence for a continued physical engagement of the Gα- and Gβγ-subunits upon binding by GTPγS or $[AlF_4]^-$. The results corroborate the hypothesis that activated heterotrimeric G proteins undergo internal structural rearrangements, rather than complete physical dissociation, during GTP turnover. This “functional dissociation” would expose potential effector-binding surfaces on each of the subunits to allow for downstream signaling, regulation, and rapid re-formation of the inactive heterotrimer upon GTP hydrolysis. The lipid bilayer is expected to play a key role in these signaling hubs both as an orienting scaffold and a modulator of each protein’s conformational landscapes.

Declarations

Acknowledgements: This work was supported by the Canadian Institutes of Health Research (CIHR) Operating Grant MOP-43998 to R.S.P., CIHR Operating Grant PJT-159464 to O.P.E. and N.V.E., the National Institute of General Medical Sciences grants GM106990 and GM083118 to R.K.S. S.K.H. was supported by Alexander Graham Bell Canada Graduate Scholarship-Doctoral from NSERC. A.S. was supported by CREST, Japan Science and Technology Agency (JST), Japan, JPMJCR1402. We thank Dmitry Pichugin for NMR maintenance and Lu Chen for technical support.

Author contributions: S.K.H and R.S.P. designed the research. S.K.H. and R.S.M.R. carried out expression and purification of various $G_s\alpha$ constructs. S.K.H. carried out expression and purification of $A_{2A}R$. S.K.H and A.P. carried out expression and purification of Gβγ. N.V.E., R.S.M.R., and S.K.H. carried out cloning for the various $G_s\alpha$ constructs. S.K.H. and R.S.M.R. performed the NMR experiments and the GTP hydrolysis experiments. A.S. performed the RTA analysis. R.K.S. provided assistance with data interpretation and the manuscript. S.K.H and R.S.P prepared the manuscript. R.S.P. and O.P.E. supervised the project.

Declaration of interests: The authors declare no competing interests.

Materials And Methods

Protein cloning, expression, and purification

Cloning of the wild type $G_s\alpha$ construct has been described previously (Huang et al., 2022). The human GNAS2 gene was subcloned into a pET15b vector immediately downstream of an open reading frame for hexahistidine-tagged maltose binding protein (MBP) and tobacco etch virus (TEV) cleavage site. The ΔCys construct (C3S, C200T, C237S, C359I, C365A, C379V) and additional single-cysteine mutants (ΔCys-K34C, ΔCys-R61C, ΔCys-Y358C, ΔCys-E370C) were generated via site-directed mutagenesis using the pET15b-$G_s\alpha$ wild type or ΔCys plasmid as a template. All mutations were confirmed by DNA sequencing at the Centre for Applied Genomics (TCAG), the Hospital for Sick Children (Toronto, Canada).

The expression and purification of $G_s\alpha$ (identical for the wild type and all mutant constructs) has been described previously (Huang et al., 2021). Briefly, *Escherichia coli* (*E. coli*) BL21 (DE3) cells containing the vector carrying the desired $G_s\alpha$ construct were grown in LB Miller medium at 25 °C to an optical density at 600 nm (OD_{600}) of 0.3. Cells were induced overnight at 19 °C with isopropyl β-d-1-thiogalactopyranoside (IPTG) to a final concentration of 50 μM, then harvested by centrifugation at 6,000 g. Cell pellets were resuspended lysis buffer (50 mM sodium phosphate, pH 8.0, 300 mM NaCl, 10 mM imidazole, 50 μM GDP, 2 mM $MgCl_2$, 0.5 mM TCEP, 5 mM 6-aminocaproic acid, 5 mM benzamidine, 0.4 mg/mL lysozyme, 2 μg/mL DNase I, 10% glycerol) and lysed via sonication. The lysate was centrifuged at 20,000 g for 30 minutes, and the resulting supernatant was incubated with TALON resins (Takara Bio) for 3 h at 4 °C with gentle mixing. For ^{19}F labeling, the TALON resins were washed with 3 bed-volumes of labeling buffer (50 mM HEPES, pH 7.4, 100 mM NaCl, 2 mM $MgCl_2$, 0.5 mM TCEP, 10% glycerol), then resuspended in 2 bed-volumes of labeling buffer containing 200 μM 2-bromo-N-(4-(trifluoromethyl)phenyl)acetamide (BTFMA, Apollo Scientific). The reaction was allowed to proceed overnight at 4 °C with gentle mixing. A second

aliquot of BTFMA was added and incubated for 6 h prior to loading the resin onto a gravity column. The resins were washed with lysis buffer containing 20 mM imidazole, then eluted with elution buffer (50 mM sodium phosphate (pH 8.0), 100 mM NaCl, 50 μM GDP, 2 mM $MgCl_2$, 0.5 mM TCEP, 10% glycerol, 250 mM imidazole). The eluted MBP-G_sα was buffer exchanged using a centrifugal filter to remove imidazole, then incubated with 10 μg/mL of TEV protease (produced in-house) at 4 °C overnight without agitation. The sample was loaded onto a Ni-NTA column and the flow-through was collected and purified on a HiLoad 16/600 Superdex 200 prep grade size exclusion column equilibrated with 50 mM HEPES, pH 7.4, 100 mM NaCl, 2 mM $MgCl_2$, 5 μM GDP, and 10% glycerol. The eluted fractions containing G_sα were pooled, concentrated, and buffer-exchanged to final storage buffer (50 mM HEPES, pH 7.4, 100 mM NaCl, 2 mM $MgCl_2$, 100 μM GDP, 10% glycerol). The proteins are flash-frozen in liquid nitrogen and stored at -80 °C until needed.

Gβγ, and $A_{2A}R$ were expressed and purified as previously described (Huang et al., 2021). Empty nanodiscs were prepared as previously described (Huang et al., 2022). Both the $A_{2A}R$ and the empty nanodiscs were reconstituted using the MSPΔH5 membrane scaffold protein (Hagn et al., 2013) and a 3:2 ratio of 1-palmitoyl-2-oleoyl-sn-glycero-3-phosphocholine (POPC) to 1-palmitoyl-2-oleoyl-sn-glycero-3-phospho-(1'-rac-glycerol) (POPG). The protein or nanodisc samples were flash-frozen in liquid nitrogen and stored at -80 °C in the following storage buffers until use. For Gβγ: 50 mM HEPES, pH 7.4, 100 mM NaCl, 2 mM $MgCl_2$, 0.0125% n-Dodecyl β-D-maltoside (DDM), 100 μM TCEP, 100 μM GDP, 10% glycerol. For $A_{2A}R$ and empty nanodiscs: 50 mM HEPES, pH 7.4, 100 mM NaCl.

NMR experiments

The purified protein stocks, stored in their respective storage buffers as described above, were combined such that the final NMR sample contained 30-80 μM BTFMA-labeled G_sα. The samples were supplemented with a final concentration of 10% D_2O and 20 μM sodium trifluoroacetate (TFA) as the ^{19}F chemical shift reference. 1.2-fold excess of Gβγ, 3-fold excess of $A_{2A}R$, or 3.5-fold excess of empty nanodiscs, relative to the G_sα concentration, were added where applicable. Where needed, the sample also contained a final concentration of 100 μM GDP (GDP or GDP-AlF_4^- conditions), 50 μM $AlCl_3$ and 5 mM NaF (GDP-$[AlF_4]^-$ conditions), 2 U/mL apyrase (nucleotide-free conditions), 2 U/mL apyrase and 1 mM GTPγS (GTPγS conditions), or 1 mM NECA ($A_{2A}R$ + NECA conditions). We note that by itself, nucleotide-free Gα is unstable and tend to aggregate within an hour at concentrations suitable for an NMR experiment. In the presence of membrane, Gβγ, or receptor, samples are stable for at least several hours to several days depending on the mutant and the temperature of storage. We also note that due to large quantities of proteins that would be required, NMR of the G_sαβγ+$A_{2A}R$+NECA+GTPgS condition was only carried out for the K34C construct. All samples were prepared in Shigemi tubes with a final volume of 200-350 μL. NMR experiments were acquired at 20 °C on either a 600 MHz Varian Inova spectrometer equipped with a ^{19}F-tunable triple-resonance cryoprobe or a 500 MHz Varian Inova spectrometer equipped with a 5 mm room temperature inverse HFX probe. A typical 1D fluorine experiment included a

100-300 ms recycle delay, a 5.5-7 µs (45°) excitation pulse, and a 500-600 ms acquisition time. Each experiment was acquired using 24,000-200,000 scans, yielding a S/N of approximately 30-100. Spectra were processed using MestReNova (Mestrelab Research S.L.) employing chemical shift referencing (-75.6 ppm for TFA), zero filling, baseline correction, and exponential apodization equivalent to a 20-30 Hz line broadening.

GTP hydrolysis assays

GTP hydrolysis assays were performed using the GTPase-Glo^{TM} assay kit (Promega, Madison, WI, USA) following the manufacturer's protocol (Mondal et al., 2015). Reactions were carried out at room temperature in a buffer containing 50 mM HEPES, pH 7.4, 100 mM NaCl, 2 mM $MgCl_2$, 10% glycerol, 1 µM GDP, and 4 µM GTP. Each reaction contained either $G_s\alpha$ alone (250 nM), $G_s\alpha\beta\gamma$ (250 nM $G_s\alpha$ + 300 nM $G\beta\gamma$), or $G_s\alpha\beta\gamma$ with $A_{2A}R$ (250 nM $G_s\alpha$ + 300 nM $G\beta\gamma$ + 250 nM $A_{2A}R$ + 100 µM NECA). All reaction mixtures were pre-incubated for 1 hour prior to the addition of GTP, which initiated the reaction. A control was also carried out with only buffer and no G protein. After 90 minutes, unhydrolyzed GTP was converted to ATP and detected using a reagent containing luciferase. The resulting luminescence is proportional to the amount of unreacted GTP and measured using a TECAN Spark multi-mode plate reader with an integration time of 1 minute. The amount of GTP hydrolysis for each condition (x) can be represented by its difference in luminescence with the control:

$$\Delta Lum_x = Lum_0 - Lum_x$$

where Lum_0 is the luminescence signal intensity of the control reaction.

Relative GTP hydrolysis for each condition (x) was calculated in relation to the wild type $G_s\alpha$.

$$Relative\ GTP\ hydrolysis\ = \frac{\Delta Lum_x}{\Delta Lum_{WT}} \times 100$$

Computational rigidity-transmission allostery predictions

Starting with the structure of GDP-bound $G_s\alpha\beta\gamma$ heterotrimer (PDB: 6EG8), we measured the allosteric propensity from the GDP binding pocket across the complex by applying rigidity-transmission allostery (RTA) analysis (Sljoka, 2021). The RTA algorithm, whose details have been previously described (Sljoka, 2021; Ye et al., 2018), is a computational tool based on the mathematical rigidity theory which identifies allosteric networks within structures of proteins and protein complexes (Jacobs et al., 2001; Sljoka, 2021; Whiteley, 2005, Ye 2018, Mehrabi 2019). The algorithm was verified with NMR chemical shift data and predicts how changes in the conformational flexibility of one region in the protein are transmitted to distal sites by quantifying the resulting regiospecific change in conformational degrees of freedom. We applied the RTA algorithm on the GDP-bound $G_s\alpha\beta\gamma$ heterotrimer by rigidifying the bound GDP. The available conformational degrees of freedom were quantified for each residue before and after GDP rigidification.

The resulting change in degrees of freedom was then extracted for each residue and represents the extent of allosteric transmission from the GDP binding pocket.

References

1. Abdulaev NG, Ngo T, Ramon E, Brabazon DM, Marino JP, Ridge KD. 2006. The receptor-bound “empty pocket” state of the heterotrimeric G-protein α-subunit is conformationally dynamic. Biochemistry **45**:12986–12997. doi:10.1021/bi061088h
2. Abdulaev NG, Ngo T, Zhang C, Dinh A, Brabazon DM, Ridge KD, Marino JP. 2005. Heterotrimeric G-protein α-subunit adopts a “preactivated” conformation when associated with βγ-subunits. J Biol Chem **280**:38071–38080. doi:10.1074/jbc.M505259200
3. Adjobo-Hermans MJW, Goedhart J, van Weeren L, Nijmeijer S, Manders EMM, Offermanns S, Gadella TWJ. 2011. Real-time visualization of heterotrimeric G protein Gq activation in living cells. BMC Biol **9**:32. doi:10.1186/1741-7007-9-32/FIGURES/7
4. Bünemann M, Frank M, Lohse MJ. 2003. Gi protein activation in intact cells involves subunit rearrangement rather than dissociation. Proc Natl Acad Sci U S A **100**:16077–16082. doi:10.1073/PNAS.2536719100
5. Chung KY, Rasmussen SGF, Liu T, Li S, Devree BT, Chae PS, Calinski D, Kobilka BK, Woods VL, Sunahara RK. 2011. Conformational changes in the G protein Gs induced by the β2 adrenergic receptor. Nature **477**:611–617. doi:10.1038/nature10488
6. Coleman DE, Berghuis AM, Lee E, Linder ME, Gilman AG, Sprang SR. 1994. Structures of active conformations of Gi alpha 1 and the mechanism of GTP hydrolysis. Science (80-) **265**:1405–1412. doi:10.1126/SCIENCE.8073283
7. Coleman DE, Sprang SR. 1998. Crystal Structures of the G Protein Giα1 Complexed with GDP and Mg2+: A Crystallographic Titration Experiment. Biochemistry **37**:14376–14385. doi:10.1021/BI9810306
8. Danielson MA, Falke JJ. 1996. Use of 19F NMR to probe protein structure and conformational changes. Annu Rev Biophys Biomol Struct **25**:163–195. doi:10.1146/annurev.bb.25.060196.001115
9. Digby GJ, Sethi PR, Lambert Nevin A, Lambert N A. 2008. Differential dissociation of G protein heterotrimers. J Physiol **586**:3325–3335. doi:10.1113/jphysiol.2008.153965
10. Dror RO, Mildorf TJ, Hilger D, Manglik A, Borhani DW, Arlow DH, Philippsen A, Villanueva N, Yang Z, Lerch MT, Hubbell WL, Kobilka BK, Sunahara RK, Shaw DE. 2015. Structural Basis for Nucleotide Exchange in Heterotrimeric G Proteins. Science (80-) **348**:1361–1365.
11. Du Y, Duc NM, Rasmussen SGF, Hilger D, Kubiak X, Wang L, Bohon J, Kim HR, Wegrecki M, Asuru A, Jeong KM, Lee J, Chance MR, Lodowski DT, Kobilka BK, Chung KY. 2019. Assembly of a GPCR-G protein complex. Cell **177**:1232–1242.e11. doi:10.1016/j.cell.2019.04.022
12. Flock T, Ravarani CNJ, Sun D, Venkatakrishnan AJ, Kayikci M, Tate CG, Veprintsev DB, Babu MM. 2015. Universal allosteric mechanism for Gα activation by GPCRs. Nature **524**:173–179.

doi:10.1038/nature14663

13. Galés C, Van Durm JJJ, Schaak S, Pontier S, Percherancier Y, Audet M, Paris H, Bouvier M. 2006. Probing the activation-promoted structural rearrangements in preassembled receptor-G protein complexes. Nat Struct Mol Biol **13**:778–786. doi:10.1038/nsmb1134
14. García-Nafría J, Lee Y, Bai X, Carpenter B, Tate CG. 2018. Cryo-EM structure of the adenosine A2A receptor coupled to an engineered heterotrimeric G protein. Elife **7**:1–19. doi:10.7554/eLife.35946.001
15. Goricanec D, Hagn F. 2019. NMR backbone and methyl resonance assignments of an inhibitory G-alpha subunit in complex with GDP. Biomol NMR Assign **13**:131–137. doi:10.1007/s12104-018-9865-9
16. Goricanec D, Stehle R, Egloff P, Grigoriu S, Plückthun A, Wagner G, Hagn F. 2016. Conformational dynamics of a G-protein α subunit is tightly regulated by nucleotide binding. Proc Natl Acad Sci **113**:E3629–E3638. doi:10.1073/pnas.1604125113
17. Hagn F, Etzkorn M, Raschle T, Wagner G. 2013. Optimized phospholipid bilayer nanodiscs facilitate high-resolution structure determination of membrane proteins. J Am Chem Soc **135**:1919–1925. doi:10.1021/ja310901f
18. Ham D, Ahn D, Ashim J, Cho Y, Kim HR, Yu W, Chung KY. 2021. Conformational switch that induces GDP release from Gi. J Struct Biol **213**:107694. doi:10.1016/j.jsb.2020.107694
19. Hamm HE. 1998. The Many Faces of G Protein Signaling. J Biol Chem **273**:669–672. doi:10.1074/JBC.273.2.669
20. Herrmann R, Heck M, Henklein P, Hofmann KP, Ernst OP. 2006. Signal transfer from GPCRs to G proteins: Role of the Gα N-terminal region in rhodopsin-transducin coupling. J Biol Chem **281**:30234–30241. doi:10.1074/jbc.M600797200
21. Hillenbrand M, Schori C, Schöppe J, Plückthun A. 2015. Comprehensive analysis of heterotrimeric G-protein complex diversity and their interactions with GPCRs in solution. Proc Natl Acad Sci U S A **112**:E1181–E1190. doi:10.1073/PNAS.1417573112/-/DCSUPPLEMENTAL
22. Hu J, Wang Y, Zhang X, Lloyd JR, Li JH, Karpiak J, Costanzi S, Wess J. 2010. Structural basis of G protein–coupled receptor–G protein interactions. *Nat Chem Biol 2010 67* **6**:541–548. doi:10.1038/nchembio.385
23. Huang SK, Almurad O, Pejana RJ, Morrison ZA, Pandey A, Picard L-P, Nitz M, Sljoka A, Prosser RS. 2022. Allosteric modulation of the adenosine A2A receptor by cholesterol. Elife **11**:e73901. doi:10.7554/eLife.73901
24. Huang SK, Pandey A, Tran DP, Villanueva NL, Kitao A, Sunahara RK, Sljoka A, Prosser RS. 2021. Delineating the conformational landscape of the adenosine A2A receptor during G protein coupling. Cell **184**:1884–1894.e14. doi:10.1016/j.cell.2021.02.041
25. Iiri T, Herzmark P, Nakamoto JM, Dop C Van, Bourne HR. 1994. Rapid GDP release from Gs alpha in patients with gain and loss of endocrine function. Nature **371**:164–168. doi:10.1038/371164A0

26. Jacobs DJ, Rader AJ, Kuhn LA, Thorpe MF. 2001. Protein flexibility predictions using graph theory. Proteins Struct Funct Genet **44**:150–165. doi:10.1002/prot.1081
27. Johnston CA, Willard MD, Kimple AJ, Siderovski DP, Willard FS. 2008. A sweet cycle for Arabidopsis G-proteins: Recent discoveries and controversies in plant G-protein signal transduction. Plant Signal Behav **3**:1067–1076. doi:10.4161/PSB.3.12.7184
28. Kano H, Toyama Y, Imai S, Iwahashi Y, Mase Y, Yokogawa M, Osawa M, Shimada I. 2019. Structural mechanism underlying G protein family-specific regulation of G protein-gated inwardly rectifying potassium channel. Nat Commun **10**:2008. doi:10.1038/s41467-019-10038-x
29. Kaya AI, Lokits AD, Gilbert JA, Iverson TM, Meiler J, Hamm HE. 2014. A conserved phenylalanine as a relay between the α5 helix and the GDP binding region of heterotrimeric Gi protein α subunit. J Biol Chem **289**:24475–24487. doi:10.1074/jbc.M114.572875
30. Kim K, Paulekas S, Sadler F, Gupte TM, Ritt M, Dysthe M, Vaidehi N, Sivaramakrishnan S. 2021. β2-adrenoceptor ligand efficacy is tuned by a two-stage interaction with the Gαs C terminus. Proc Natl Acad Sci U S A **118**:1–11. doi:10.1073/pnas.2017201118
31. Klein S, Reuveni H, Levitzki A. 2000. Signal transduction by a nondissociable heterotrimeric yeast G protein. Proc Natl Acad Sci U S A **97**:3219–3223. doi:10.1073/PNAS.050015797
32. Kleuss C, Krause E. 2003. Gαs is palmitoylated at the N-terminal glycine. EMBO J **22**:826–832. doi:10.1093/EMBOJ/CDG095
33. Knight KM, Ghosh S, Campbell SL, Lefevre TJ, Olsen RHJ, Smrcka A V., Valentin NH, Yin G, Vaidehi N, Dohlman HG. 2021. A universal allosteric mechanism for G protein activation. Mol Cell **81**:1384–1396.e6. doi:10.1016/j.molcel.2021.02.002
34. Linder ME, Middleton P, Hepler JR, Taussig R, Gilman AG, Mumby SM. 1993. Lipid modifications of G proteins: alpha subunits are palmitoylated. Proc Natl Acad Sci **90**:3675–3679. doi:10.1073/PNAS.90.8.3675
35. Liu X, Xu X, Hilger D, Aschauer P, Tiemann JKS, Du Y, Liu H, Hirata K, Sun X, Guixà-González R, Mathiesen JM, Hildebrand PW, Kobilka BK. 2019. Structural Insights into the Process of GPCR-G Protein Complex Formation. Cell **177**:1243–1251.e12. doi:10.1016/j.cell.2019.04.021
36. Medkova M, Preininger AM, Yu NJ, Hubbell WL, Hamm HE. 2002. Conformational changes in the amino-terminal helix of the G protein αi1 following dissociation from Gβγ subunit and activation. Biochemistry **41**:9962–9972. doi:10.1021/bi0255726
37. Mondal S, Hsiao K, Goueli SA. 2015. A homogenous bioluminescent system for measuring GTPase, GTPase activating protein, and guanine nucleotide exchange factor activities. Assay Drug Dev Technol **13**:444–455. doi:10.1089/adt.2015.643
38. Oldham WM, Van Eps N, Preininger AM, Hubbell WL, Hamm HE. 2006. Mechanism of the receptor-catalyzed activation of heterotrimeric G proteins. Nat Struct Mol Biol **13**:772–777. doi:10.1038/nsmb1129
39. Posner BA, Mixon MB, Wall MA, Gilman AG, Sprang SR. 1998. The A326S mutant of Gialpha1 as an approximation of the receptor-bound state. J Biol Chem **273**:21752–21758.

doi:10.1074/JBC.273.34.21752

40. Qi C, Sorrentino S, Medalia O, Korkhov VM. 2019. The structure of a membrane adenylyl cyclase bound to an activated stimulatory G protein. Science (80-) **364**:389–394. doi:10.1126/science.aav0778
41. Rasmussen SGF, DeVree BT, Zou Y, Kruse AC, Chung KY, Kobilka TS, Thian FS, Chae PS, Pardon E, Calinski D, Mathiesen JM, Shah STA, Lyons JA, Caffrey M, Gellman SH, Steyaert J, Skiniotis G, Weis WI, Sunahara RK, Kobilka BK. 2011. Crystal structure of the β2 adrenergic receptor–Gs protein complex. Nature **477**:549–555. doi:10.1038/nature10361
42. Rebois RV, Robitaille M, Galés C, Dupré DJ, Baragli A, Trieu P, Ethier N, Bouvier M, Hébert TE. 2006. Heterotrimeric G proteins form stable complexes with adenylyl cyclase and Kir3.1 channels in living cells. J Cell Sci **119**:2807–2818. doi:10.1242/JCS.03021
43. Ridge KD, Abdulaev NG, Zhang C, Ngo T, Brabazon DM, Marino JP. 2006. Conformational changes associated with receptor-stimulated guanine nucleotide exchange in a heterotrimeric G-protein α-subunit: NMR analysis of GTPγS-bound states. J Biol Chem **281**:7635–7648. doi:10.1074/jbc.M509851200
44. Sljoka A. 2021. Probing Allosteric Mechanism with Long-Range Rigidity Transmission Across Protein Networks. Methods Mol Biol **2253**:61–75. doi:10.1007/978-1-0716-1154-8_5
45. Smrcka A V., Kichika N, Tarragó T, Burroughs M, Park MS, Itoga NK, Stern HA, Willardson BM, Giralt E. 2010. NMR analysis of G-protein βγ subunit complexes reveals a dynamic Gα-Gβγ subunit interface and multiple protein recognition modes. PNAS **107**:639–644. doi:10.1073/pnas.0909503107
46. Sondek J, Lambright DG, Noel JP, Hamm HE, Sigler PB. 1994. GTPase mechanism of Gproteins from the 1.7-Å crystal structure of transducin α-GDP-AIF – 4. Nature **372**:276–279. doi:10.1038/372276A0
47. Sprang SR. 2016. Activation of G proteins by GTP and the mechanism of Gα-catalyzed GTP hydrolysis. Biopolymers **105**:449–462. doi:10.1002/bip.22836
48. Sunahara RK, Tesmer JJG, Gilman AG, Sprang SR. 1997. Crystal structure of the adenylyl cyclase activator G(sα). Science (80-) **278**:1943–1947. doi:10.1126/SCIENCE.278.5345.1943
49. Tang W, Tu Y, Nayak SK, Woodson J, Jehl M, Ross EM. 2006. Gβγ inhibits Gα GTPase-activating proteins by inhibition of Gα-GTP binding during stimulation by receptor. J Biol Chem **281**:4746–4753. doi:10.1074/jbc.M510573200
50. Thomas TC, Schmidt CJ, Neer EJ. 1993. G-protein alpha o subunit: mutation of conserved cysteines identifies a subunit contact surface and alters GDP affinity. Proc Natl Acad Sci **90**:10295–10299. doi:10.1073/PNAS.90.21.10295
51. Toyama Y, Kano H, Mase Y, Yokogawa M, Osawa M, Shimada I. 2017. Dynamic regulation of GDP binding to G proteins revealed by magnetic field-dependent NMR relaxation analyses. Nat Commun **8**:14523. doi:10.1038/ncomms14523
52. Traut TW. 1994. Physiological concentrations of purines and pyrimidines. Mol Cell Biochem **140**:1–22. doi:10.1007/BF00928361

53. Tsutsumi R, Fukata Y, Noritake J, Iwanaga T, Perez F, Fukata M. 2009. Identification of G protein alpha subunit-palmitoylating enzyme. Mol Cell Biol **29**:435–447. doi:10.1128/MCB.01144-08
54. Van Eps N, Preininger AM, Alexander N, Kaya AI, Meier S, Meiler J, Hamm HE, Hubbell WL. 2011. Interaction of a G protein with an activated receptor opens the interdomain interface in the alpha subunit. Proc Natl Acad Sci U S A **108**:9420–9424. doi:10.1073/pnas.1105810108
55. Wang S, Assmann SM, Fedoroff N V. 2008. Characterization of the Arabidopsis Heterotrimeric G Protein. J Biol Chem **283**:13913–13922. doi:10.1074/JBC.M801376200
56. Westfield GH, Rasmussen SGF, Su M, Dutta S, DeVree BT, Chung KY, Calinski D, Velez-Ruiz G, Oleskie AN, Pardon E, Chae PS, Liu T, Li S, Woods VL, Steyaert J, Kobilka BK, Sunahara RK, Skiniotis G. 2011. Structural flexibility of the Gαs α-helical domain in the β2-adrenoceptor Gs complex. PNAS **108**:16086–16091. doi:10.1073/pnas.1113645108
57. Whiteley W. 2005. Counting out to the flexibility of molecules. Phys Biol **2**:S116–S126.
58. Wittinghofer A. 1997. Signaling mechanistics: Aluminum fluoride for molecule of the year. Curr Biol **7**:R682–R685. doi:10.1016/S0960-9822(06)00355-1
59. Ye L, Neale C, Sljoka A, Lyda B, Pichugin D, Tsuchimura N, Larda ST, Pomès R, García AE, Ernst OP, Sunahara RK, Prosser RS. 2018. Mechanistic insights into allosteric regulation of the A2A adenosine G protein-coupled receptor by physiological cations. Nat Commun **9**. doi:10.1038/s41467-018-03314-9
60. Ye L, Van Eps N, Zimmer M, Ernst OP, Scott Prosser R. 2016. Activation of the A2A adenosine G-protein-coupled receptor by conformational selection. Nature **533**:265–268. doi:10.1038/nature17668
61. Yin J, Chen KYM, Clark MJ, Hijazi M, Kumari P, Bai X chen, Sunahara RK, Barth P, Rosenbaum DM. 2020. Structure of a D2 dopamine receptor–G-protein complex in a lipid membrane. Nature **584**:125–129. doi:10.1038/s41586-020-2379-5

Figures

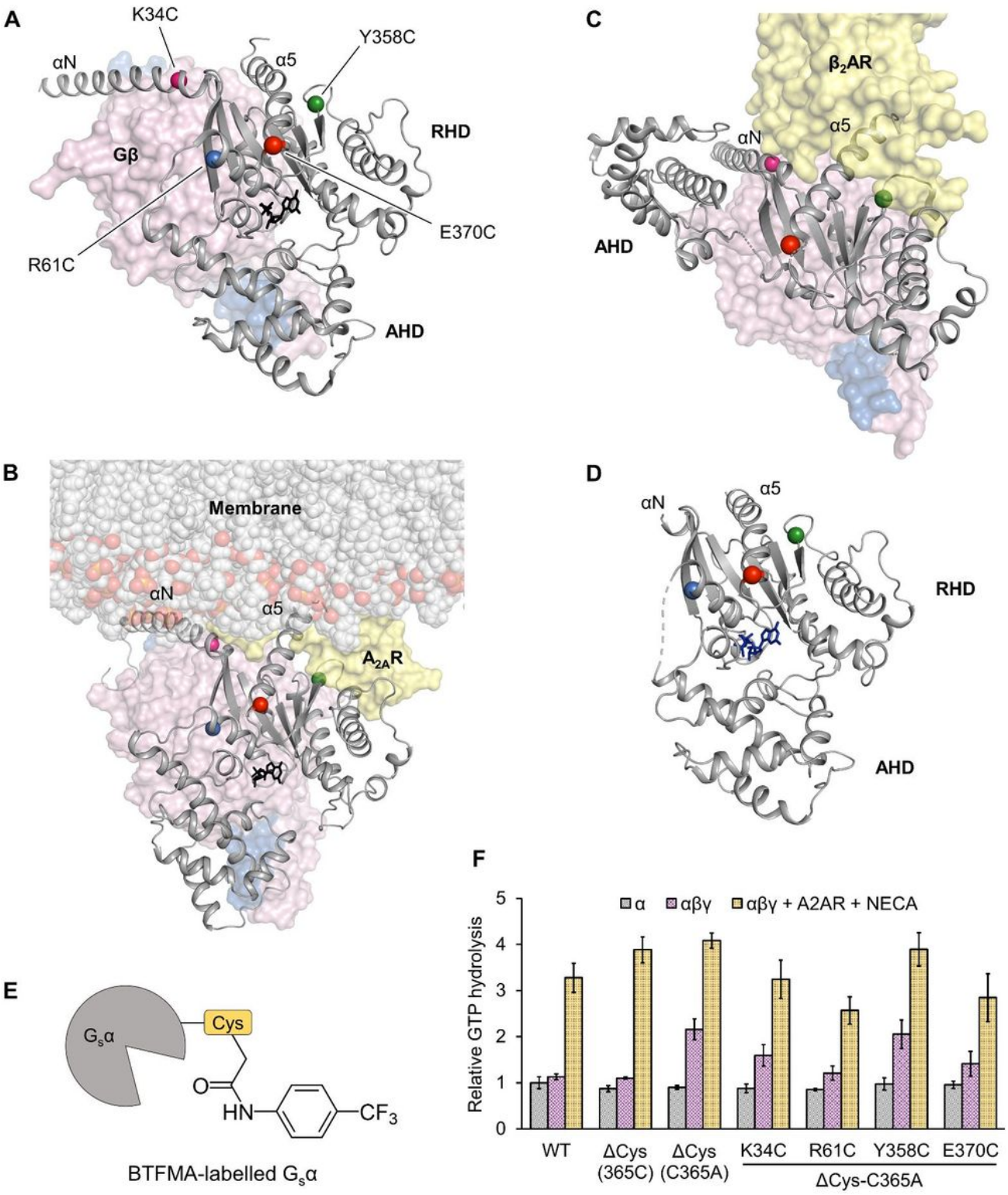

Figure 1

Labeling sites for probing the conformational landscape of $G_s\alpha$. (A) Crystal structure of $G_s\alpha\beta\gamma$•GDP (PDB: 6EG8) showing the labeling site α-carbons as spheres. Four residues within the RHD of $G_s\alpha$ (coloured grey) were selected for cysteine substitution and ^{19}F-labeling: K34C on helix N (αN), R61C on helix 1 (α1), Y358C on the α4β6 loop, and E370C at the junction between the β6α5 loop and helix 5 (α5). **(B)** A model

obtained from (Huang et al., 2021) of G_sαβγ•GDP in complex with NECA-bound A_{2A}R in a lipid bilayer. The labeling site α-carbons are shown as spheres using the same colours as in panel **A**. **(C)** Crystal structure of the nucleotide-free G_sαβγ complexed with the β_2-adrenergic receptor (PDB: 3SN6). All labeling sites are shown as spheres except for R61, which belongs to a region of missing electron density. **(D)** Crystal structure of G_sα•GTPγS (PDB: 1AZT). Residue K34 is missing in this structure due to missing electron density from a disordered αN helix. In panels **A**-**D**, Gβ (pink), Gγ (blue), and receptor (yellow) are shown as surfaces, GDP is shown in black sticks, GTPγS is shown in navy sticks, and phospholipids are represented in spheres. **(E)** Schematic of the ^{19}F reporter, BTFMA. **(F)** Cumulative GTP hydrolysis by various G_sα mutants in a 90-minute period relative to wild type (WT) G_sα. The reactions contain either G_sα alone, G_sαβγ, or G_sαβγ with A_{2A}R bound to the agonist NECA. Data represent mean ± SEM (n = 4).

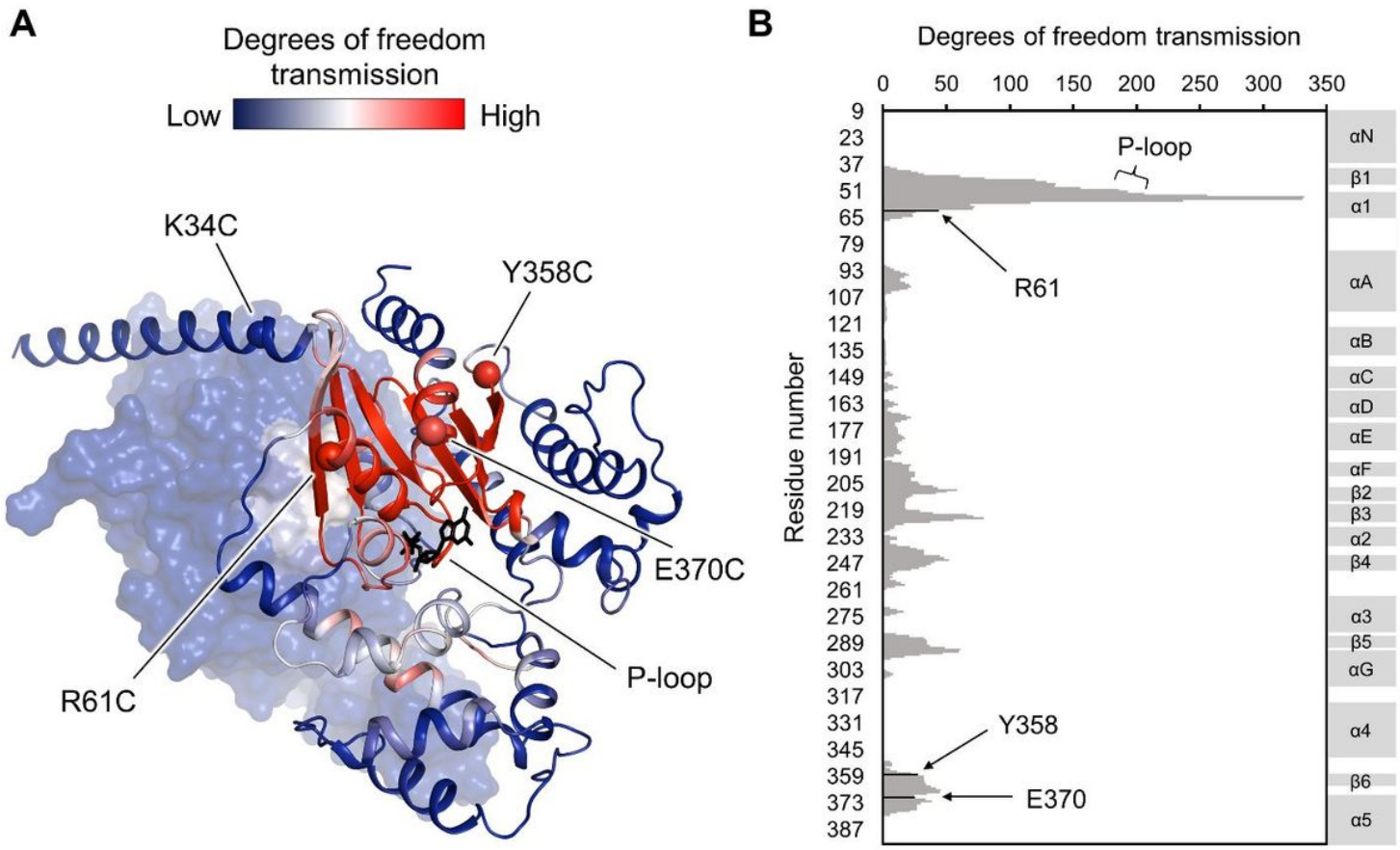

Figure 2

Three out of four labeling sites are allosterically engaged with bound GDP. (A) RTA analysis of G_sαβγ (PDB: 6EG8) revealed an allosteric network upon the rigidification of GDP (black sticks). The intensity of allosteric transmission from the bound GDP is measured by the change in degrees of freedom at each atom and is mapped in colour (red/blue gradient bar). **(B)** Degrees of freedom transmission is plotted for each residue in G_sα.

Figure 3

$G_s\alpha$ reveals a complex landscape characterized by both global and local conformational dynamics. ^{19}F NMR spectra of BTFMA-labeled $G_s\alpha$ as a function of membrane (empty nanodiscs), Gβγ, nucleotide (GDP, GTPγS, or nucleotide-free (NF)), and $A_{2A}R$ (apo or NECA-bound). Two global conformational states, denoted A and B, are identified across all four labeling sites (red and green stripes). Nucleotide-free conditions were achieved via the addition of apyrase.

Figure 4

Distinct conformational signatures are observed for the N-terminal helix in the combined presence of Gβγ and $A_{2A}R$. (A) Overlay of the crystal structures of $G_s\alpha\beta\gamma$•GDP (grey, PDB: 6EG8), nucleotide-free $G_s\alpha\beta\gamma$ complexed with the β_2-adrenergic receptor (orange, PDB: 3SN6), and $G_s\alpha$•GTPγS (green, PDB: 1AZT) focusing on the K34C labeling site on αN (α-carbons represented as spheres). The Gβ subunit (pink) and the receptor (yellow) from 3SN6 are shown as surfaces. The Gβ subunit from 6EG8 is omitted for clarity. **(B)** ^{19}F NMR spectra of BTFMA-labeled $G_s\alpha$-K34C either alone, together with Gβγ and membrane, with NECA-bound $A_{2A}R$, or in the joint presence of both Gβγ and $A_{2A}R$. The red and green dashed lines denote the global A state and B state, respectively. Two additional resonances (indicated by asterisksasterisks) are stabilized upon the binding of GTPγS in the context of the ternary complex (top spectrum). A distinct downfield resonance is also observed in the combined presence of Gβγ and $A_{2A}R$. This is denoted the “sandwiched state” and marked by the grey dashed box.

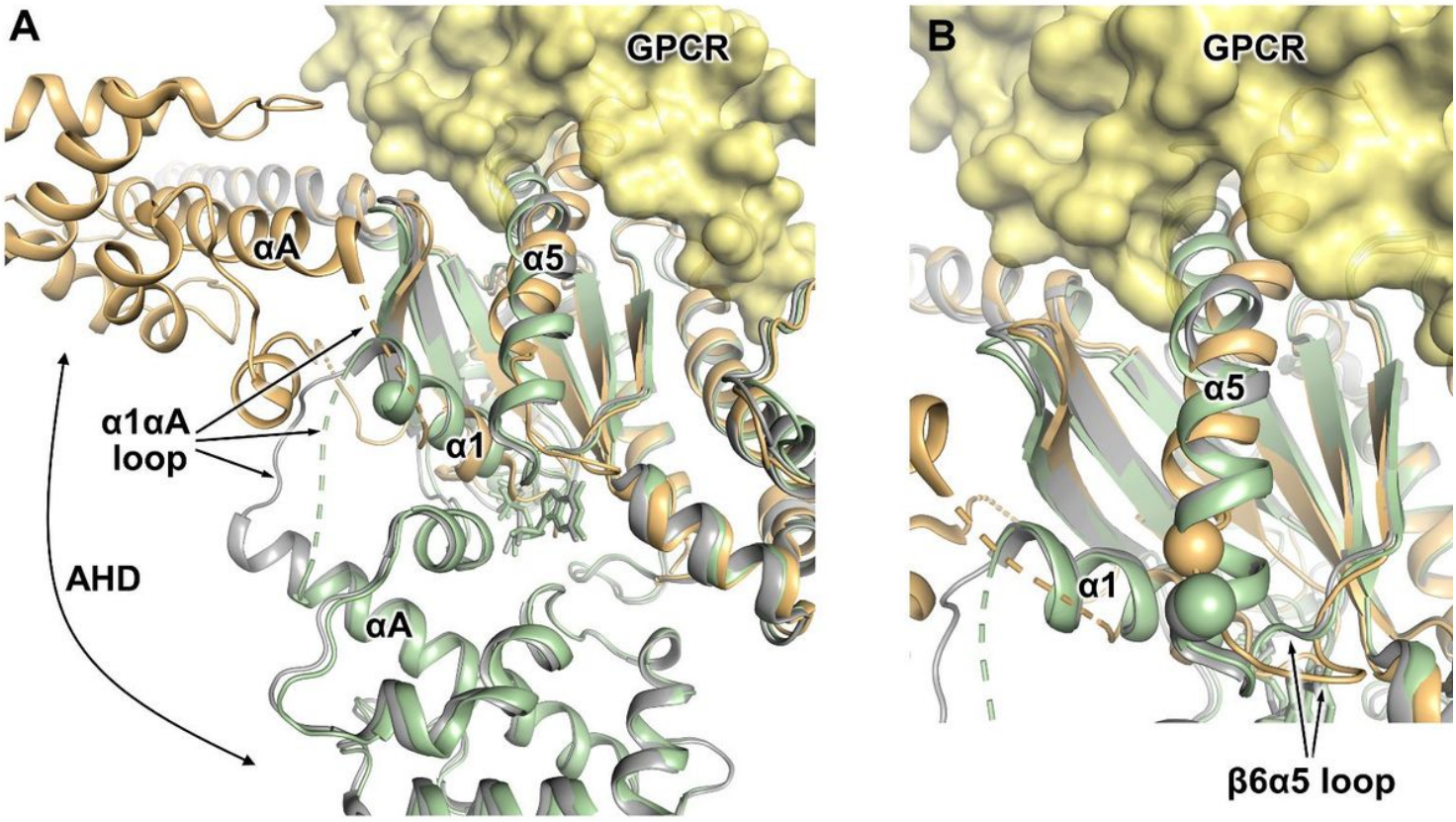

Figure 5

Hinge region connecting the RHD and the AHD undergoes order-disorder transitions upon nucleotide release. Overlay of the crystal structures of G_sαβγ•GDP (grey, PDB: 6EG8), nucleotide-free G_sαβγ complexed with the β_2-adrenergic receptor (orange, PDB: 3SN6), and G_sα•GTPγS (green, PDB: 1AZT) highlighting R61 on the α1 helix **(A)** and E370 on the α5 helix **(B)**. The α-carbons associated with the labeled residues are represented as spheres. The receptor is shown in a yellow surface representation and the Gβγ subunits are omitted for clarity. Disordered regions with missing electron density are shown as dashed loop segments.

Figure 6

Y358C exhibits chemical shift sensitivity toward nucleotide. (A) ^{19}F NMR spectra of BTFMA-labeled G_sα-Y358C as a function of nucleotide (GDP or GTPγS), membrane (empty nanodiscs), and Gβγ. The two red lines denoting the global A state are separated in chemical shift based on whether GDP or GTPγS is present. In contrast, the global B state (green dashed line) is not sensitive to the identity of the bound nucleotide. The addition of Gβγ without empty nanodiscs is sufficient at shifting the equilibrium toward B, suggesting that this pose is allosterically induced and not a result of direct membrane interaction. **(B)**

Structural overlay of G_sαβγ•GDP (grey, PDB: 6EG8), nucleotide-free G_sαβγ complexed with the β_2-adrenergic receptor (orange, PDB: 3SN6), and G_sα•GTPγS (green, PDB: 1AZT) highlighting the Y358C labeling site (α-carbons represented as spheres). The Gβ subunit (pink) and the receptor (yellow) from 3SN6 are shown as surfaces. The Gβ subunit from 6EG8 is omitted for clarity.

Figure 7

The G_sαβγ heterotrimer undergoes structural rearrangement rather than complete physical dissociation in the presence of GDP-$[AlF_4]^-$ and GTPγS. ^{19}F NMR spectra of BTFMA-labeled G_sα in the presence of GDP, GDP-$[AlF_4]^-$, and GTPγS. Spectra were acquired for G_sα alone, G_sα with membrane (empty nanodiscs), and G_sαβγ with membrane. The two global states, A and B, are highlighted with red and green stripes respectively.